

Preparation of Gelatin/Polyvinyl alcohol decorated with WO_3 for cartilage regeneration

Kevin Catzim-Ríos¹, Cintya Soria-Hernández¹, María R. Rocha-Pizaña^{2,1} and Wendy Ortega-Lara^{1*}.

¹ Tecnológico de Monterrey, Escuela de Ingeniería y Ciencias, Ave. Eugenio Garza Sada 2501, Monterrey 64849, NL, Mexico.

² Tecnológico de Monterrey, NatProLab, Department of Bioengineering, School of Engineering and Science, Av. Atlixécayotl 5718, C.P.72453 Puebla, Puebla, México.

* Corresponding Authors

Abstract— *Research-based learning offers a stimulating approach to understanding bone regeneration. Students can formulate research questions, such as optimizing biomaterial design for enhanced healing. This delves into the current body of knowledge on bone structure, growth factors, and biocompatible materials. A Student for eight semesters of Nanotechnology Engineering collaborating with a master's Nanotechnology student at Tec de Monterrey was selected to be trained and develop a theoretical and experimental frame on new alternatives in hydroxyapatite for bone regeneration. Ceramic particles have been widely used in developing new materials with biomedical applications. However, no material has been found that can match the properties of natural tissues and organs, so considering the evaluation of different ceramic particles for biological fines could help meet the current needs of the materials to be developed. Tungsten trioxide (WO_3) is a peculiar ceramic particle since various investigations have shown that, in addition to its use in piezoelectric devices, it has anti-carcinogenic properties at low concentrations and promotes bioactivity on the surfaces of inert materials. In this document, WO_3 nanoparticles have been synthesized by an acid precipitation method supported by a hydrothermal treatment. The obtained particles were used to evaluate their cytotoxicity using a cell viability test in cell lines belonging to fibroblasts and osteoblasts. The best concentration was 31 $\mu\text{g/ml}$. On the other hand, at the concentrations used, WO_3 did not increase cell death. Instead, it promoted bioactivity, so it is presented as a material that could be used with biomedical applications. This fosters a profound understanding of bone biology, the complexities of regeneration, and the potential solutions researchers are exploring.*

Keywords— *Research-based learning, higher education, Nanotechnology, educational innovation, Tungsten Oxide, Hydrogel, Bioactivity*

I. INTRODUCTION

Through research-based learning, students engage in hands-on exploration, critical analysis of scientific literature, and collaborative problem-solving to address the multifaceted challenges within the field¹. Moreover, research-based learning promotes interdisciplinary collaboration, encouraging students to draw from diverse fields such as biology, engineering, and materials science to innovate novel bone repair and regeneration strategies as presented. In this case, undergraduate and master students worked and collaborated in state-of-the-art, and the main discussions are as follows.

The limited regeneration potential of different cells in the human body creates an ample opportunity in tissue engineering. The development of scaffolds that promote cell adhesion and match the chemical and mechanical properties of the native tissue is a challenge in undergoing research. The requirements for these scaffolds are complex: biocompatibility, adequate mechanical parameters, and non-toxic and non-inflammatory biodegradation components are needed in the host organism¹.

Hydrogels are biomaterials attractive scaffolds as their 3D structures are made of natural macromolecules and synthetic polymers upon crosslinking methods².

Tungsten trioxide is a chemical compound from oxygen and the transition metal tungsten. Recent studies on medical applications suggest WO_3 conjugated nanoparticles is an antibacterial and tissue promoter agent given by their electrochromic and photochromic properties³.

Ultrasonically prepared tungsten oxide-graphene oxide (WO_3 -GO) nanocomposite photocatalytic efficiency was compared with that of pure WO_3 nanoparticles, and the results indicate better performance as a photocatalyst, antibacterial and anticancer system⁴⁻⁶.

Conjugating WO_3 with hydrogel is expected to enable better semiconductor and sensing characteristics. In other words, the combination of hydrogel and WO_3 nanoparticles is expected to give a better-combining recognition target ability and biocompatibility without toxicity. Tungsten particles were synthesized by precipitation technique.

II. MATERIALS AND METHODS

Sodium tungstate dihydrate ($\text{Na}_2\text{WO}_4 \cdot 2\text{H}_2\text{O}$, 99%), poly(vinyl-alcohol) ($[-\text{CH}_2\text{CHOH}-]_n$, M_w 85,000-124,000, 99+%), gelatin from cold water fish, magnesium chloride hexahydrate ($6(\text{MgCl}_2 \cdot 6\text{H}_2\text{O})$, 99-102%), calcium chloride anhydrous (CaCl_2 , $\geq 93\%$), trizma base ($\text{NH}_2\text{C}(\text{CH}_2\text{OH})_3$, $\geq 99.9\%$), sodium chloride (NaCl , 99%), potassium chloride (KCl , 99-100.5%) and dibasic phosphate potassium (K_2HPO_4 , $\geq 98\%$) were purchased from Sigma-Aldrich (St. Louis, MO, USA). In addition, nitric acid (HNO_3 , 64.2%), absolute ethanol ($\text{CH}_3\text{CH}_2\text{OH}$, 99.83%), hydrochloric acid (HCl , 36.5- 38%), sodium bicarbonate (NaHCO_3 , 100.188%), and sodium sulfate anhydrous (Na_2SO_4 , $\geq 99\%$) were purchased from CTR Scientific.

A. Tungsten Oxide (WO_3) Synthesis

The acid precipitation technique reported by Vamvasakis, *et al*, was used to synthesize tungsten oxide. 0.667 g of $\text{Na}_2\text{WO}_4 \cdot 2\text{H}_2\text{O}$ (99% Sigma-Aldrich) were weighed into a 50 mL beaker, and then 20 mL of deionized water was added and stirred for 10 min to eventually leave the solution at rest until it took on a translucent appearance. Then, concentrated hydrochloric acid HCL was added dropwise with constant stirring until the solution became a notable yellow-transparent color. The solution was placed under hydrothermal treatment at 95 °C for 24 h to form a white-yellow precipitate. Finally, the supernatant was discarded, and the solid was calcined at 500 °C/5 h.

B. Formulation of Hydrogel matrix of Poly((vinyl alcohol) and Gelatin

A 10% PVA solution was prepared, and the necessary amount of gelatin was slowly added under constant stirring to obtain a weight-volume concentration of 2.5% m/v. The solution was heated at 80 °C/1 h, checked for undissolved gelatin lumps, and cooled. Finally, the casting method was used to prepare the samples. For the crosslinking process, freeze-thaw cycles were performed where the samples were frozen at -20 °C/3 h and then thawed at room temperature for four h. This cycle was repeated three times.

C. Cell Viability Assay

Three different WO_3 particles embedded in hydrogels were evaluated. Different concentrations were prepared for each particle: 500, 250, 125, and 31 $\mu\text{g}/\text{mL}$. The prepared solutions were placed in 5 mL syringes, and, using a 21G needle, small drops of the gels were placed in several Petri dishes. The drops were subjected to the freeze-thaw process at -20 °C and thawed

at room temperature for at least 4 h for each process. The drops were then dried in a desiccator for 24 h.

The drops average weight was found to be 0.0013 ± 0.0002 g. Then, they were exposed to UV light for 15 min to sterilize them. The gels were placed in a 96-well plate so that there were triplicates for each gel concentration. In each well with gels, 100 μL of cells were added at 2×10^4 cells/mL for both fibroblasts (NIH) and osteoblasts (HFOB). Then, 100 μL of medium was added. In addition, wells were set up specifically for cell control without embedded gels. The 96-well plate was then incubated at 37 °C/24 h. CellTiter 96 Aqueous was added and incubated for an additional 1 h. Finally, the gels were removed, and the supernatant was analyzed by spectrophotometry.

III. RESULTS

A. Synthesis of Tungsten Oxide WO_3

The diffraction pattern for the tungsten oxide powder is represented in Figure 1. The results obtained were indexed with the JCPDS crystallographic card no: 01-072-0677, where it was found that the powder obtained has a monoclinic crystalline system. The pattern is indexed to the same, and the calculated lattice parameters are $a = 7.3060 \text{ \AA}$, $b = 7.5400 \text{ \AA}$, $c = 7.6920 \text{ \AA}$, $\beta = 90.8810^\circ$, space group P21/n (14). The crystalline size (D) of the WO_3 particles was calculated from the XRD pattern using Sharrer's formula from the full-width half maximum (FWHM) value of the major intensity peaks. The value was found to be, on average, $32.566 \pm 13.995 \text{ nm}$.

On the other hand, most crystallographic planes align correctly with those shown in the previously mentioned crystallographic chart. However, some planes do not coordinate accurately, as is the case of the plane located at $2\theta = 24.299^\circ$ (d_{202}), a location where the d_{200} crystallographic plane should appear more pronounced, this may be due to having more than one phase crystalline present in the analyzed sample. This was verified by performing a Rietveld refinement, which showed that although the d_{200} plane is present, it is overlapped by the d_{202} plane belonging to another higher molecular weight tungsten oxide and to chlorine, which is present in percentages of 9.7 % and 9.6% respectively in the sample.

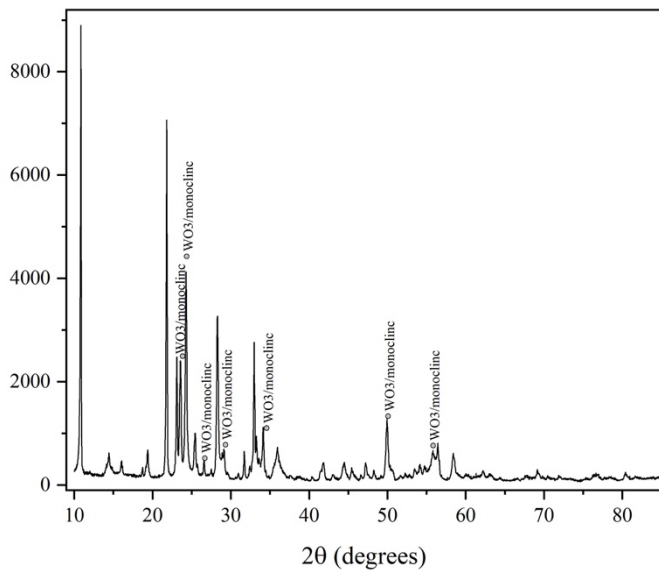


Figure 1. Diffraction pattern obtained by XRD for WO_3 synthesis.

The particle size of the tungsten oxide powder was characterized by sem. figure 2a shows distributions of particles that appear to be agglomerated, forming little porous structures. on the other hand, in figure 2b shows small particles with an average size of 130 ± 25.97 nm, and their morphology could be classified as irregular nanocrystals or with slight tendencies to platelets, such as found by the research group of Vamvasakis [1].

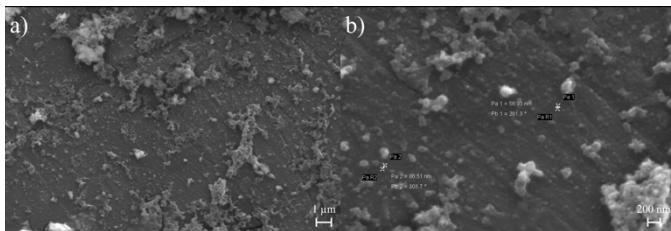


Figure 2. Scanning Electron Microscopy for synthesized WO_3 .

Figure 3 shows the FTIR results for WO_3 synthesis. The peak located at 1660 cm^{-1} corresponds to the deformation vibrations of the H-O-H bonds of water absorbed by the surface of the particles. The O-W-O stretching modes can be attributed to the peaks located at 768 and 848 cm^{-1} [2]. On the other hand, the bands located at 700 and 1516 cm^{-1} can be attributed to the presence of chlorine and higher molecular weight tungsten oxide contaminants found when analysing the diffraction pattern of the sample.

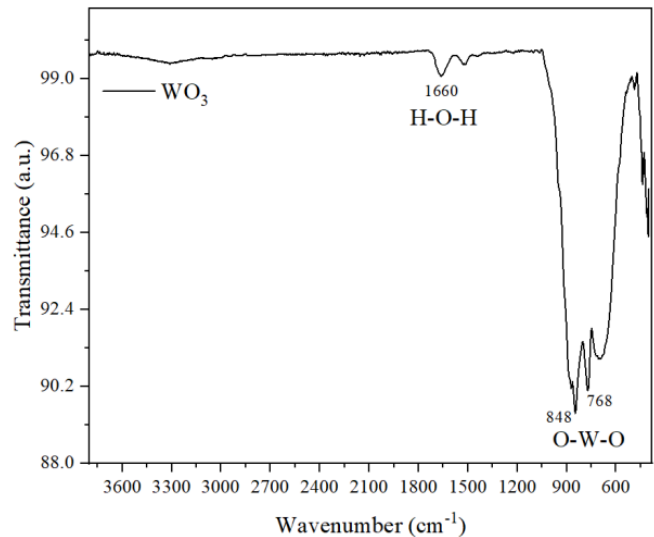


Figure 3. ATR-FTIR Spectrum for synthesized WO_3 .

Finally, EDX was used as a complementary technique to know the percentage of elements found in the obtained tungsten oxide powder. The atomic weight composition was found to be 15.47% and 84.53% of tungsten and oxygen, respectively.

B. Formulation of Hydrogel matrix of Poly((vinyl alcohol) and Gelatin

Figure 4c shows the spectrum obtained for the result of joining the PVA with Gelatin, where it can clearly be seen that it seems as if the individual spectra of both precursors were combined into one. Figure 4c a band is observed at 1540 cm^{-1} belonging to the stretching of the N-H bond of the amide group, which would indicate that esterification did not occur. The intense peak at 1640 cm^{-1} corresponds to the carbonyl group C=O, this group is permanently displaced towards lower wavenumbers when it is next to an N-H group. On the other hand, the band located at 3280 cm^{-1} in the crosslinked product was broader and more pronounced, which could give an indication of the formation of hydrogen bonds between the hydroxyl groups O-H of PVA and the amide of Gelatin [3].

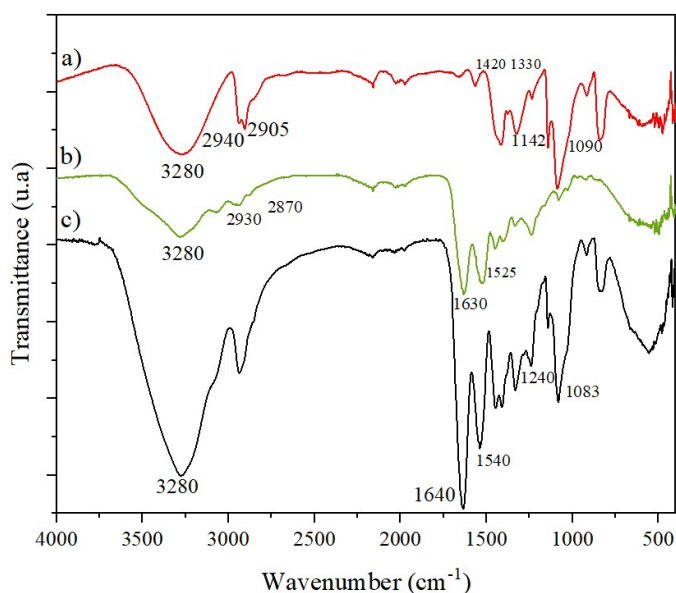


Figure 4. ATR-FTIR spectrum for hydrogel formulation a) PVA, b) Gelatin and c) PVA crosslinked Gelatin hydrogel.

C. Cell Viability Assay

Figure 5a-b shows cell viability in fibroblasts and osteoblasts, respectively. First, it can be seen that the gel without particles PVA/Gel shows about 50% dead cells after 24 h of incubation. This behavior could be due to the slightly acidic environment of 5.96 of the control group, which is outside the range for an optimal medium for cell culture survival. Tungsten oxide is a special case because the literature indicates that this compound is cytotoxic even at moderate concentrations. However, studying this compound in these formulations is of great interest since it has been shown to have antibacterial and anticancer activity [4], [5]. Thus, in Figure 5, it can be seen that statistically, considering the standard deviation, there are no significant differences between the samples and the control group. However, a slight improvement in cell viability can be seen at a concentration of 31 $\mu\text{g/mL}$, which decreases slightly as the particle concentration increases. This tendency agrees with Jeevitha, et al. in WO_3 -GO antibacterial and anticancer studies. On the other hand, adding WO_3 particles to PVA/Gel hydrogels was found to have no negative effect on cell viability.

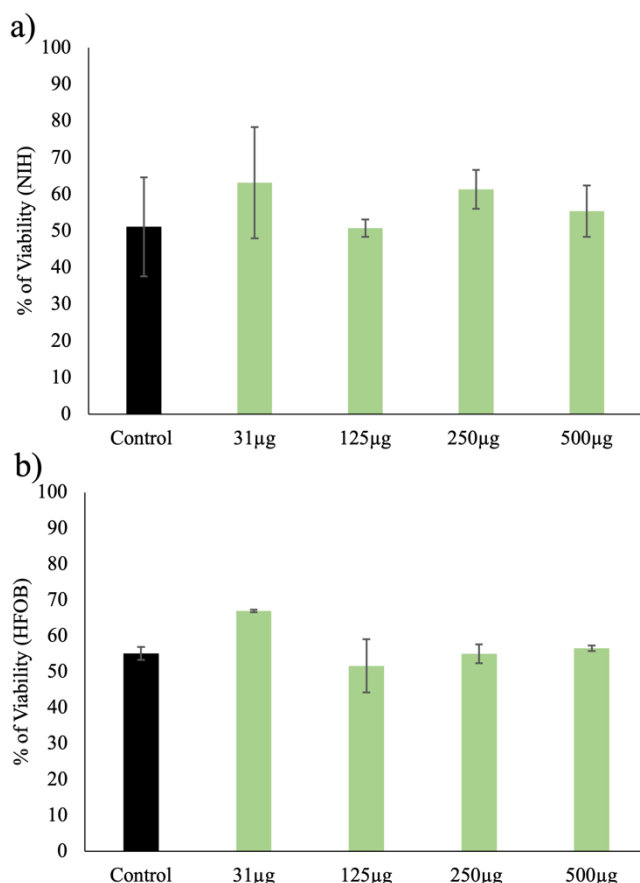


Figure 5. Cell viability assay. a) Fibroblasts (NIH). b) Osteoblasts (HF0B). * Significantly Different ($P < 0.005$), $n=3$.

D. Bioactivity Analysis

Figure 6 shows the result of the bioactivity test after 21 days. The PVA/Gel hydrogel in Figure 6a shows the deposition of a layer on the surface. However, under magnification, the presence of cubic structures can be seen, which could be related to the deposition of crystalline salts, and no bioactivity develops. On the other hand, Figure 6b shows PVA/Gel- WO_3 hydrogel with the formation of a layer with a cauliflower-like structure, which is a typical structure in the formation of apatite. Besides, the formation of apatite was confirmed by FTIR. The bands located at 560 and 600 cm^{-1} correspond to PO_4^{3-} bending ν_4 symmetry; those characteristic peaks are in agreement with Klee et al., and indicate the possible formation of different forms of apatite: fluorapatite, hydroxyapatite, chlorapatite, among others.

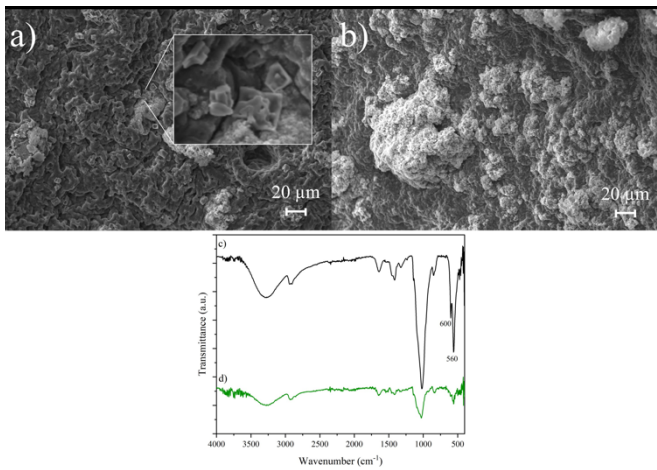


Figure 6. Bioactivity analysis. a) PVA/Gel control. b) PVA/Gel-WO₃. c) Bioactivity PVA/Gel FTIR. d) Bioactivity PVA/Gel-WO₃.

E. Cell-Hydrogel Adhesion

Figure 7 shows the adhesion of cells to the hydrogel surface. Figure 7a-b show the PVA/gel hydrogel and cells without hydrogel control groups, respectively. It can be seen a rough hydrogel surface with few cells deposited, which is consistent with the low percentage of cell viability in the previous section. However, in Figure 7c-e, there is an increase in the number of cells deposited on the hydrogel surface, which is consistent with cell viability at a concentration of 31 μg/mL. On the other hand, when the particle concentration was increased to 500 μg/mL in Figure 7d-f, the presence of cells decreases abruptly.

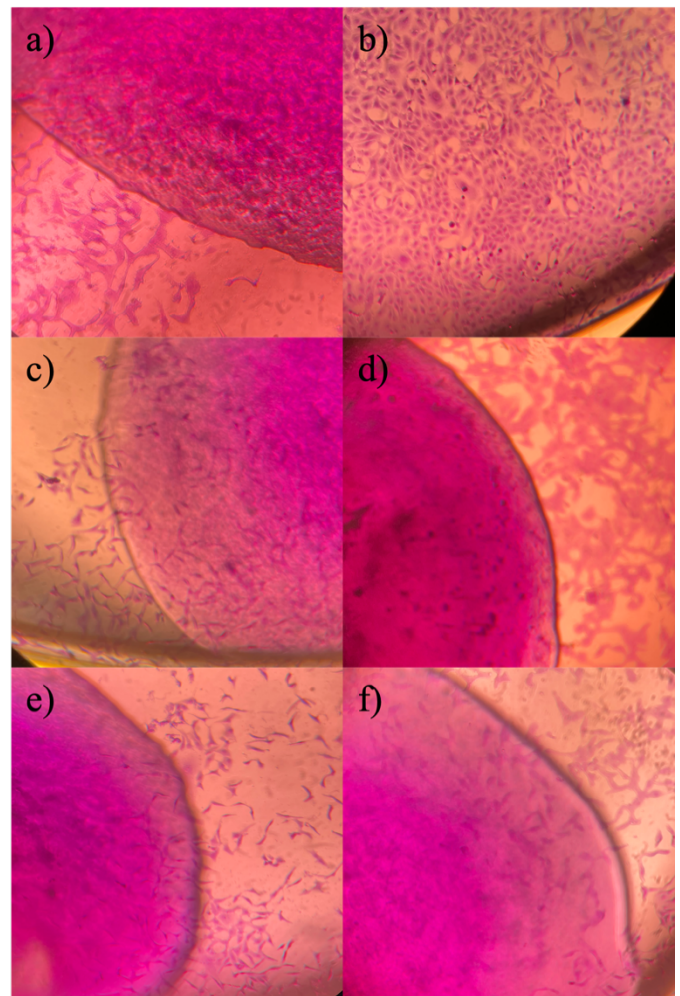


Figure 7. Cell adhesion. a) Cell-PVA/Gel. b) Cells without hydrogels. c) NIH-PVA/Gel-WO₃ at 31 μg/mL. d) NIH-PVA/Gel-WO₃ at 500 μg/mL. e) HFOB-PVA/Gel-WO₃ at 31 μg/mL. f) HFOB-PVA/Gel-WO₃ at 500 μg/mL.

IV. CONCLUSION

This study investigated the potential application of hydrogel-based tungsten trioxide (WO₃) particle integration for cartilage scaffolds. The research addressed challenges in tissue engineering, especially in cartilage regeneration, due to the limited regenerative capacity of human cells. WO₃-loaded hydrogel scaffolds were designed to replicate native tissue characteristics.

The synthesis of WO₃ particles was successfully achieved through the acid precipitation method, with an average size of 130 ± 25.97 nm and monoclinic crystalline structures. The crystallographic features, morphology, composition, and integrity of the WO₃ particles were confirmed through characterization using XRD, SEM, FTIR, and EDX.

The hydrogel matrix, composed of gelatin and poly(vinyl alcohol), demonstrated promising properties for cartilage tissue engineering. The ATR-FTIR spectra indicated the formation of hydrogen bonds between gelatin's amide groups and PVA's hydroxyl groups in the crosslinked hydrogel. The hydrogel

exhibited bioactivity, forming apatite-like structures confirmed by FTIR.

Cell viability assays demonstrated that the addition of WO₃ particles, especially at a concentration of 31 µg/mL, did not negatively impact cell viability, a significant finding given the reported cytotoxicity of tungsten oxide. The hybrid hydrogel-WO₃ scaffold holds promise for tissue engineering, potentially promoting cell survival.

Bioactivity investigations validated the deposition of apatite-like structures on the PVA/Gel-WO₃ hydrogel, indicating its potential to support tissue regeneration. Cell-hydrogel adhesion experiments revealed increased cell adhesion at lower particle concentrations (31 µg/mL), emphasizing the importance of optimizing WO₃ concentration for enhanced cellular interaction.

In conclusion, incorporating tungsten trioxide particles into a hydrogel matrix represents a viable approach to creating cartilage scaffolds. The hybrid hydrogel-WO₃ scaffold exhibited favorable characteristics, including bioactivity and cell compatibility. To advance this strategy towards practical applications in cartilage tissue engineering, further optimization of WO₃ concentration and in vivo research are essential.

This research-based learning and collaboration solidifies foundational knowledge and ignites curiosity and bone problem-solving skills, potentially leading to future breakthroughs in bone regeneration therapies. Under grade biomaterials, students were motivated and had an early engagement in theoretical discussions. This educational approach cultivates a new generation of scientists and postgrad students developing projects equipped with the knowledge, skills, and creativity to advance the forefront of bone regeneration research. It could improve clinical outcomes for patients worldwide.

ACKNOWLEDGMENT

The authors would like to acknowledge the financial support of Writing Lab, Institute for the Future of Education, Tecnológico de Monterrey, Mexico, in producing this work".

This research was supported by the Monterrey Institute of Technology, Monterrey, Mexico, and Kevin Catzim's postgraduate scholarship from the National Council of Humanities, Sciences, and Technologies (CONNECT) and Monterrey Institute of Technology and Higher Education.

REFERENCES

[1] Bowyer, D. M., Akpınar, M., Erdogan, A., Malik, K., & Horkey, F. (2022). Mobilizing Research-Based Learning (RBL) in Higher Education: International Perspectives From Three Institutions. In *Handbook of Research on*

Active Learning and Student Engagement in Higher Education, pp. 246-269, 2022. doi: 10.4018/978-1-7998-9564-0.ch012

- [2] Vamvasakis, I. Georgaki, D. Vernardou, G. Kenanakis, and N. Katsarakis, "Synthesis of WO₃ catalytic powders: evaluation of photocatalytic activity under NUV/visible light irradiation and alkaline reaction pH," *J Solgel Sci Technol*, vol. 76, no. 1, pp. 120–128, Oct. 2015, doi: 10.1007/S10971-015-3758-5/FIGURES/6.
- [3] P. J. Boruah, R. R. Khanikar, and H. Bailung, "Synthesis and Characterization of Oxygen Vacancy Induced Narrow Bandgap Tungsten Oxide (WO_{3-x}) Nanoparticles by Plasma Discharge in Liquid and Its Photocatalytic Activity," *Plasma Chemistry and Plasma Processing*, vol. 40, no. 4, pp. 1019–1036, Jul. 2020, doi: 10.1007/S11090-020-10073-3/FIGURES/11.
- [4] A Ávila-Ramirez, K Catzim-Ríos, E. Guerrero-Beltral, E. Ramírez Cedillo, W. Ortega-Lara, "Reinforcement of Alginate-Gelatin Hydrogels with Bioceramics for Biomedical Applications: A Comparative Study," *Gels* (7), no. 4, October 21, doi: <https://doi.org/10.3390/gels7040184>
- [5] N. Leawhiran, P. Pavasant, K. Soontornvipart, and P. Supaphol, "Gamma irradiation synthesis and characterization of AgNP/gelatin/PVA hydrogels for antibacterial wound dressings," *J Appl Polym Sci*, vol. 131, no. 23, Dec. 2014, doi: 10.1002/APP.41138.
- [6] Ensoylu, M., Deliormanlı, A.M. & Atmaca, H. Tungsten disulfide nanoparticle-containing PCL and PLGA-coated bioactive glass composite scaffolds for bone tissue engineering applications. *J Mater Sci* **56**, 18650–18667 (2021). <https://doi.org/10.1007/s10853-021-06494-w>
- [7] Ensoylu, M., Atmaca, H. & Deliormanlı, A.M. Fabrication and in vitro characterization of macroporous WS₂/ bioactive glass scaffolds for biomedical applications. *J Aust Ceram Soc* **58**, 397–409 (2022). <https://doi.org/10.1007/s41779-021-00696-w>